

Gapless edge states and their stability in two-dimensional quantum magnets

Takafumi Suzuki¹ and Masahiro Sato²

¹*Research Center for Nano-Micro Structure Science and Engineering,*

Graduate School of Engineering, University of Hyogo, Himeji, Hyogo 671-2280, Japan

²*Department of Physics and Mathematics, Aoyama Gakuin University, Sagamihara, Kanagawa 229-8558, Japan*

(Dated: September 22, 2018)

We study the nature of edge states in extrinsically and spontaneously dimerized states of two-dimensional spin- $\frac{1}{2}$ antiferromagnets, by performing quantum Monte Carlo simulation. We show that a gapless edge mode emerges in the wide region of the dimerized phases, and the critical exponent of spin correlators along the edge deviates from the value of Tomonaga-Luttinger (TL) liquid universality in large but finite systems at low temperatures. We also demonstrate that the gapless nature at edges is stable against several perturbations such as external magnetic field, easy-plane XXZ anisotropy, Dzyaloshinskii-Moriya interaction, and further-neighbor exchange interactions. The edge states exhibit non TL-liquid behavior, depending strongly on model parameters and kinds of perturbations. Possible ways of detecting these edge states are discussed. Properties of edge states we show in this paper could also be used as reference points to study other edge states of more exotic gapped magnetic phases such as spin liquids.

PACS numbers: 75.10.Jm, 75.10.Pq, 75.10.Kt, 73.43.-f, 75.10.-b

I. INTRODUCTION

In recent years, gapful ground states without any *local* order parameter and their boundary properties have been vividly studied in quantum many-body physics from both theoretical and experimental viewpoints. Among such disordered states, two-dimensional (2D) and three-dimensional (3D) topological insulators (TIs), for instance, have attracted much attention as novel many-body phases in solids.^{1,2} Their fundamental properties are that the bulk has a finite excitation gap, but its boundary (surface or edge) is metallic (i.e., gapless) and around the boundary, up-spin electrons move antiparallel to the motion of down-spin electrons (this nature is called helical). This gapless boundary state is quite stable against any perturbation with time-reversal symmetry, and the existence of a helical edge mode is recorded in a \mathbb{Z}_2 topological invariant defined on the bulk (bulk-edge correspondence).

In quantum spin systems, the Haldane-gap state³ is also famous as a state without any local order. This state is defined as the ground state of one-dimensional (1D) spin-1 antiferromagnetic (AF) chains and is actually realized in some quasi-1D magnets.^{4,5} Its characteristic features can be captured by a valence-bond solid (VBS) picture.⁶ Namely, the Haldane state can be approximated by the uniform tensor product state of local singlet dimers composed of two fictitious $S = \frac{1}{2}$ spins on neighboring sites, which are generated via the decomposition of original $S = 1$ spin on each site. From the solid singlet distribution, we can easily understand the existence of a finite excitation gap (called the Haldane gap) on the Haldane state. Similarly, the uniform alignment of singlets indicates the absence of any local order parameter, but we can construct a *non-local* string order parameter⁷ to distinguish the Haldane state from the other paramagnetic phases. The VBS picture also shows

that an almost free $S = \frac{1}{2}$ spin appears at the edge of the finite-size spin-1 Haldane state under free boundary condition.⁵ In addition to these results, recently new ways of characterizing the Haldane states have been actively discussed based on symmetries and artificial quantities such as entanglement spectra.⁸⁻¹⁰

All of the gapped, topological phases in free fermion systems including TI have been successfully classified theoretically.¹¹⁻¹³ On the other hand, topological phases and boundary states in quantum spin systems have been less understood, except for a few VBS (such as the Haldane state) and short-range valence-bond states in 1D spin systems including spin ladders. Therefore, the understanding of topological nature and boundary properties in quantum spin systems, especially, in *higher-dimensional* magnets, is an important, fundamental issue in magnetism. One might image VBS¹⁴ or exotic spin-liquid states as typical examples of 2D or 3D gapped non-magnetic spin states with a gapless edge mode. It is, however, difficult to prepare such states in nature because the corresponding Hamiltonians contain various tuned coupling constants. In addition, usual magnetic ordered states such as Néel and spiral ordered states are not suitable since both edge and bulk are trivially gapless due to the Nambu-Goldstone mode. Instead of these states, simple, realistic systems with both a gapless edge mode and a bulk gap would be suitable for starting to understand edge modes in 2D and 3D spin systems. In this paper, we thus study the nature of edge modes in 2D spin-Peierls (dimerized) states, by using the quantum Monte Carlo (QMC) method based on the worm algorithm.¹⁵⁻¹⁷

There is a similarity between TIs and the Haldane state: A finite bulk gap, gapless boundary states, and the \mathbb{Z}_2 topological invariant of TI seem to correspond to a Haldane gap, free edge spins, and the string order parameter of the Haldane state, respectively. We will hence

consider how the edge modes of dimerized states are different from and similar to those of TIs and the Haldane state. It would be impossible to define any topological order parameter for 2D dimerized states, and in that sense, the gapless edge states in dimerized states (even if they exist) are naively expected to be less stable compared to those of TIs. We should, however, note that it is generally hard to predict whether or not there exist gapless edge states and how stable they are, since quantum spin systems we consider below are strongly correlated systems that are different from free fermion models for TIs.

The rest of this paper is organized as follows. In Sec. II, we explain two kinds of 2D quantum AF models with an extrinsically or intrinsically dimerized phase. Both models can be analyzed by using QMC techniques. In Sec. III, we briefly summarize characteristic features of correlation functions of the standard Tomonaga-Luttinger (TL) liquid phase in purely 1D critical AF spin systems before the analysis of two spin-Peierls models. The properties of TL liquid are useful for discussing the edge states in the dimerized phase. Section. IV is devoted to our numerical analysis and is the main content of this paper. We show in Sec. IV A that a gapless edge mode really exists in the dimer phases of both models, and the critical exponent of the spin-correlation function along the edge moves away from the value of standard TL liquid in the weakly dimerized region. We then discuss the stability of the gapless edge mode against realistic perturbations in Sec. IV B. We demonstrate that the gapless nature survives after introducing several perturbations with different symmetries, while the edge critical exponents drastically change depending on the kinds of perturbations. We briefly consider some experimental ways of observing gapless edge modes in Sec. V. Finally, we summarize our numerical results and predictions in Sec. VI.

II. MODEL

Dimerized phases are roughly classified into an extrinsically dimerized phase without any spontaneous symmetry breaking (SSB) and an intrinsically dimerized one with a spontaneous translational symmetry breaking. To study those two states we utilize two $SU(2)$ -symmetric spin- $\frac{1}{2}$ AF models on a square lattice defined in the x - y plane: the dimerized model^{18,19} and the JQ_3 model.²⁰ Their Hamiltonians are given as

$$\mathcal{H}_{\text{dim}} = \sum_{\langle i,j \rangle} J \mathbf{S}_i \cdot \mathbf{S}_j + \sum_j J \alpha \delta_{j_y, \text{even}} \mathbf{S}_j \cdot \mathbf{S}_{j+\mathbf{e}_y}, \quad (1a)$$

$$\mathcal{H}_{JQ_3} = \sum_{\langle i,j \rangle} J \mathbf{S}_i \cdot \mathbf{S}_j + \sum_{\langle i,j,k,l,m,n \rangle} Q_3 C_{ij} C_{kl} C_{mn} \quad (1b)$$

where \mathbf{S}_j is the spin- $\frac{1}{2}$ operator on site $j = (j_x, j_y)$ ($j_{x,y} \in \mathbb{Z}$), $\mathbf{e}_{x[y]} = (1, 0)$ [(0, 1)] is the unit vector for the x [y] direction, $J > 0$ is the AF exchange coupling constant between neighboring spins, and $C_{ij} = 1/4 - \mathbf{S}_i \cdot \mathbf{S}_j$. In the dimerized model (1a), α denotes the magnitude

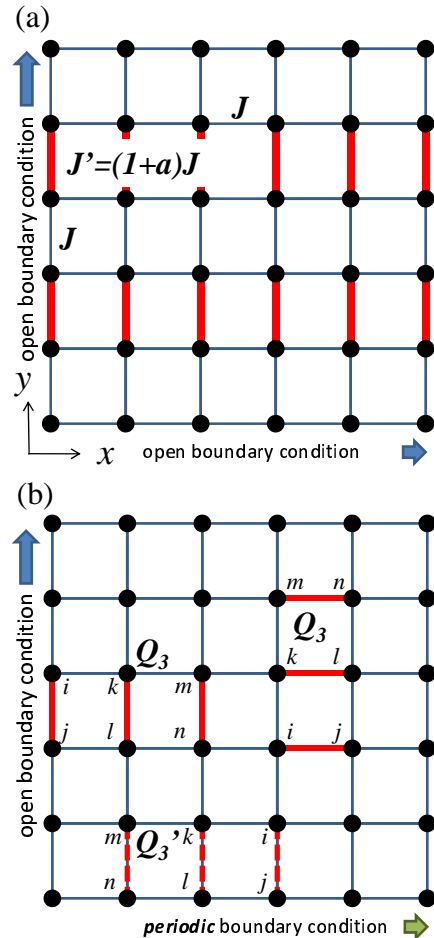


FIG. 1. (color online) (a) 2D dimerized model with bond alternation along the y direction. (b) 2D JQ_3 model with six-spin interaction term. The modified coupling constant Q'_3 on edges is explained in Sec. II.

of external dimerization along the y direction as shown in Fig. 1(a), in which the dimerized bond strength $J' = J(1 + \alpha)$. If α is strong enough and the open boundary condition for y direction is imposed as in Fig. 1, an effective spin chain is expected to appear along the x direction at the edge thanks to the formation of dimerization on all strong bonds J' . In the JQ_3 model (1b), the second Q_3 term includes six-spin interactions, where six sites (i, j, k, l, m, n) are defined on two neighboring plaquettes (rectangle) shown in Fig. 1(b). The symbol $\sum_{\langle i,j,k,l,m,n \rangle}$ stands for the summation over all rectangles on the square lattice.

The ground-state phase diagrams for the dimerized and JQ_3 models have been investigated by QMC calculations, and both models show the Néel-dimer quantum phase transition.²¹ For the dimerized model, the critical point is located at $J' = J'_c \simeq 1.91J$ ^{18,19} and singlet dimers appear on all the bonds J' for $J' > J'_c$. The tran-

sition of the JQ_3 model takes place at $Q_3 = Q_{3c} \simeq 1.5J$ and the spins spontaneously form a columnar dimer state along the x or y direction when $Q_3 > Q_{3c}$.²⁰ It is worth noticing that the dimer phase of Eq. (1a) does not accompany any SSB similarly to TIs, while in the case of Eq. (1b), the translational symmetry is spontaneously broken.

The JQ_3 model seems to be a toy model, but it is one of the few spin models with a spontaneously dimerized phase and can be accurately analyzed by QMC simulation without a negative sign problem. Furthermore, its dimerized ground-state wave function is expected to be close enough to that of real dimerized magnets. To study possible gapless edge modes of the model (1a), we impose an open boundary condition for the y direction as shown in Fig. 1(a). On the other hand, we have confirmed from the QMC simulation that in the dimer phase of the JQ_3 model, singlet dimers tend to reside on edges when we set the open boundary condition to make the edges. For this dimerization pattern, no gapless edge state is expected. In order to remove the dimers on edges and make the same dimerization pattern as that of the dimerized model (1a), we modify the value of Q_3 to $Q'_3 (< Q_3)$ at the edge as depicted in Fig. 1(b). From QMC results of $Q'_3/Q_3 = 0.0, 0.25,$ and $0.5,$ we have checked that the resultant dimers do not reside on the edges and the nature of edge states is not sensitive for changing the value of Q'_3 . We therefore set $Q'_3/Q_3 = 0.5$ throughout this paper.

III. TOMONAGA-LUTTINGER LIQUID

In order to judge whether or not a gapless edge mode is present, we utilize two-point spin-correlation functions at the edge of two models in Eq. (1). If it exists, an algebraic decay of the correlators is expected, while the correlators decay in an exponential fashion when the edge state has a finite excitation gap. When the dimerized model approaches the limit $\alpha \rightarrow \infty$, an isolated spin- $\frac{1}{2}$ AF chain appears at the edge and its low-energy physics is governed by a gapless Tomonaga-Luttinger (TL) liquid. It is therefore important to summarize spin correlators of the TL liquid phase as a reference point before embarking on our QMC results.

For an ideal TL liquid phase of spin- $\frac{1}{2}$ AF chains, transverse and longitudinal spin correlations are known to behave as²²

$$\langle S_r^x S_0^x \rangle \sim C_1 (-1)^r r^{-\eta_{xy}} + \dots, \quad (2a)$$

$$\langle S_r^z S_0^z \rangle \sim m^2 + C_2 r^{-\eta_z} \cos(2k_F r) + \dots, \quad (2b)$$

at long distances $r \gg 1$. Here the uniform magnetization $m = \langle S_j^z \rangle$ is induced by external magnetic field H along the S^z axis, $2k_F = \pi(1-2m)$ is the "Fermi" wave number, and $C_{1,2}$ are non-universal constants. It is well known that critical exponents $\eta_{xy,z}$ satisfy the relation²²

$$\eta_{xy}\eta_z = 1 \quad (3)$$

and $\eta_{xy} = \eta_z = 1$ occurs at the $SU(2)$ -symmetric case. We also note that a $2k_F$ incommensurate oscillation disappears at $m = H = 0$ in Eq. (2b).

IV. NUMERICAL ANALYSIS

This section is the main content of the paper, and we show all the important QMC results here. We discuss numerically evaluated physical quantities, especially spin correlation functions of the two models (1a) and (1b), and the stability of their edge states. In the QMC simulation, we adopt the boundary condition of Fig. 1, and mainly consider square-shaped finite-size systems in which the lengths of x and y directions, L_x and L_y , are both fixed to L . In order to see the low-temperature physics of both models, we set temperature T proportional to L^{-1} . We note that correlation lengths and critical exponents appear in this section are all evaluated from the QMC results for fixed models with the largest size and the lowest temperature.

A. Gapless Edge States and Critical Exponents

We first discuss the spin-correlation functions in the dimer phases of the two models (1a) and (1b). Figure 2 shows numerically determined spin-correlation functions along the x direction on edge and those along the y direction at $x = L/2$ for the dimerized phases of both dimerized and JQ_3 models at sufficiently low temperatures $T \propto L^{-1}$. Hereafter, a correlation function along the x direction on the edge (along the y direction) is called edge (bulk) correlation. The long-distance behavior of edge spin correlations $S_{\mu\mu}(r_x) \equiv \langle S_{(r_x,0)}^\mu S_{(0,0)}^\mu \rangle$ is well explained by a power-law decay in both models, reflecting the existence of a gapless edge state. The critical exponent η defined by $|S_{\mu\mu}(r)| \sim r^{-\eta}$ is evaluated as $\eta \simeq 1.13$ (0.97) for the dimer (JQ_3) model. We stress that *this algebraic-decay behavior survives far from the dimer limit*. In fact, the parameters $Q_3/J = 2.5$ and $J'/J = 2$ correspond to $Q_3/Q_{3c} \simeq 1.67$ and $J'/J_c \simeq 1.05$, respectively. Furthermore, another remarkable point is that *the critical exponent η violates a TL liquid relation $\eta_{xy} = \eta_z = 1$* . We have also evaluated $\eta \simeq 1.01$ (0.99) at a more deeply dimerized point $J'/J = 5$ ($Q_3/J = 4$) in the dimerized (JQ_3) model. On the other hand, as shown in the inset of Fig. 2, the bulk spin correlations $B_{\mu\mu}(r_y) \equiv \langle S_{(L/2,r_y)}^\mu S_{(L/2,0)}^\mu \rangle$ decay exponentially, indicating a finite dimerization gap in the bulk. The correlation lengths ξ_y of $|B_{\mu\mu}(r_y)| \sim \exp[-r_y/\xi_y]$ are evaluated as $\xi_y \sim 7.4$ (4.0) for the dimerized (JQ_3) model. These large values of ξ_y clearly show that the edge chain is really correlated to the bulk. Namely, the edge correlation of Fig. 2 should be regarded as an intrinsic result of 2D models, and it should be distinguished from correlation functions in 1D systems such as spin chains and ladders. From these results, we conclude that a gapless edge state

is realized in the wide range of both extrinsically and spontaneously spin-Peierls phases, but the critical exponent deviates from that of TL liquid, especially, near the 2D transition points between dimer and Néel phases.

In the rest of this subsection, let us consider why the critical exponent η deviates from the value of the TL liquid $\eta_{xy} = \eta_z = 1$. From the renormalization-group (RG) viewpoint,^{22,23} it would be natural that the value of η approaches unity if the system is sufficiently close to the thermodynamic and zero-temperature limit. Such a tendency however cannot be observed upto the $L = 96$ system in Fig. 2. We have further checked that the exponent η gradually decreases from 1.13, but it does not reach unity in the dimerized model at $J'/J = 2$ as we increase both the edge length L_x and the inverse of temperature $J/T = L_x$ upto 256 by using rectangle-shaped systems with $L_x > L_y$. This result definitely suggests that very large sizes $L_{x,y}$ and extremely low temperatures are necessary to observe the crossover from the non-TL liquid

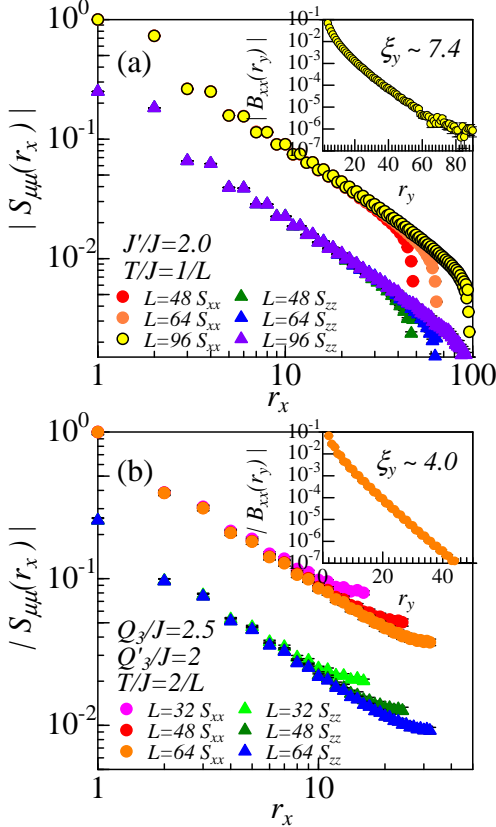


FIG. 2. (color online) Spin-spin correlation $|S_{\mu\mu}(r_x)| = |\langle S_{(r_x,0)}^\mu S_{(0,0)}^\mu \rangle|$ on the edge in the dimerized phase of (a) dimerized model and (b) JQ_3 model. Insets are the results along the bulk direction: $|B_{\mu\mu}(r_y)| = |\langle S_{(L/2,r_y)}^\mu S_{(L/2,0)}^\mu \rangle|$. We normalize the values of $|S_{xx}(1)|$ and $|B_{xx}(1)|$ to be unity. In the inset, we depict only the results for B_{xx} because of the $SU(2)$ symmetry of the models. Errors are drawn on all symbols, but they are less than the symbol size.

to the usual TL liquid in the edge correlations if we approach the dimer-Néel transition point. In other words, the RG flow to the TL liquid fixed point is expected to be extremely slow. It is well known that a quantum critical region²³ is widely expanded around the dimer-Néel quantum critical point.²⁴ The non-trivial value of η is hence expected to be attributed to effects of large fluctuations around the 2D quantum critical point. In that sense, the values η and their J'/J and Q_3/J dependence are characteristic properties of the 2D spin-Peierls systems, and they would not be observed in 1D quantum magnets such as N -leg spin ladders.

In experiments for spin-Peierls compounds, it is generally difficult to realize an extremely low temperature limit $T/J \rightarrow +0$ and a clean edge without any defect or any impurity. It is hence expected that the evaluated critical exponents $\eta \neq 1$ in large but finite systems can be relevant in real materials, in principle, rather than the value of the TL liquid $\eta_{xy,z} = 1$. We will consider how to detect the gapless edge modes in the next section. Following the above argument, we will continuously use square-shaped systems with finite-size $L \times L$ to see the experimentally expected behavior of several correlation functions throughout this section.

B. Stability against Perturbations

We next discuss how robust the gapless edge mode is against various kinds of perturbations. This is very important since the lack of stability indicates the difficulty of observing the edge state in real magnets. As realistic perturbations, we consider an uniform Zeeman term \mathcal{H}_z , a XXZ-type magnetic anisotropy \mathcal{H}_{xxz} , a Dzyaloshinskii-Moriya (DM) interaction \mathcal{H}_{DM} with DM vector $\mathbf{D}_{ij} \parallel S^z$, a next-nearest-neighbor interaction perpendicular to the edge direction $\mathcal{H}_{\text{N.N.N}}$, and an additional bond modulation for the x direction \mathcal{H}_{alt} . They are expressed as

$$\mathcal{H}_z = -H \sum_j S_j^z, \quad (4a)$$

$$\mathcal{H}_{\text{xxz}} = -J\Delta \sum_{\langle i,j \rangle} S_i^z S_j^z, \quad (4b)$$

$$\mathcal{H}_{\text{DM}} = \sum_{\langle i,j \rangle} \mathbf{D}_{ij} \cdot (\mathbf{S}_i \times \mathbf{S}_j), \quad (\mathbf{D}_{ij} \parallel S^z) \quad (4c)$$

$$\mathcal{H}_{\text{N.N.N}} = \sum_{i_x=j_x, i_y+2=j_y} E \mathbf{S}_i \cdot \mathbf{S}_j, \quad (4d)$$

$$\mathcal{H}_{\text{alt}} = J \sum_r (-1)^{r_x} \delta \mathbf{S}_r \mathbf{S}_{r+\mathbf{e}_x}, \quad (4e)$$

and some of them are depicted in Fig. 3. These perturbations possess the following nature of symmetry. The Zeeman term \mathcal{H}_z breaks time-reversal symmetry, and \mathcal{H}_{DM} breaks link-parity symmetry. These two and \mathcal{H}_{xxz} reduce the $SU(2)$ symmetry to the axial $U(1)$ type. The bond alternation term \mathcal{H}_{alt} eliminates the translational symmetry along the x direction (if we apply a periodic

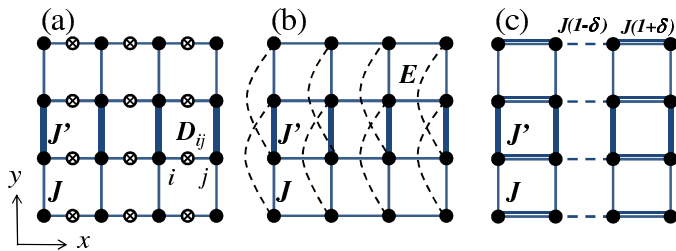


FIG. 3. (color online) Perturbations in the dimerized model: (a) DM interaction, (b) next-nearest neighbor interaction, and (c) bond alternation. Open boundary condition is imposed for both x and y directions, and the edge state appears parallel to the x direction. In the panel (a), cross circles on J bonds indicate the direction of $\mathbf{D}_{i,j}$ vector.

boundary condition). In contrast, $\mathcal{H}_{N,N,N}$ does not violate any symmetry of the original models.

1. Effect of External Magnetic Field

First let us consider the effects of the uniform magnetic field H which is one of the few things we can control. We plot the edge spin correlations and magnetization profiles in the presence of magnetic field H in Figs. 4 and 5, respectively. We have verified that the bulk correlation has a finite correlation length ξ_y under the magnetic field H , i.e., the bulk is still gapped. Figure 4 shows that even in H , a power-low decay fashion survives in the edge spin correlations, having an incommensurate oscillation in the longitudinal S^z correlation. The stability against H is in contrast to the helical edge of TIs and edge spins of Haldane states. The incommensurability is very similar to Eq. (2b), while we have checked that such an incommensurate oscillation is absent in the bulk correlations. Figure 5 reveals that a finite magnetization emerges *only around the edge* with increase of H . Finite magnetizations on multiple sites near the edge indicate that in addition to the edge spin chain, some arrays around the edge also become gapless due to a small H . This inhomogeneous magnetization profile can be observed in principle, for example, by using nuclear magnetic resonance (NMR). Both Figs. 4 and 5 clearly indicate that the gapless edge mode survives under field H .

2. Effects of Other Perturbations

Next let us consider effects of \mathcal{H}_{DM} and \mathcal{H}_{xxx} . For the JQ_3 models with the perturbations (4b)-(4e), technical difficulties of the QMC method emerge in highly accurate computations. We will therefore focus only on the dimerized model below. However effects of the perturbations on the dimerized model are probably very similar to those on the JQ_3 model since the wave functions of

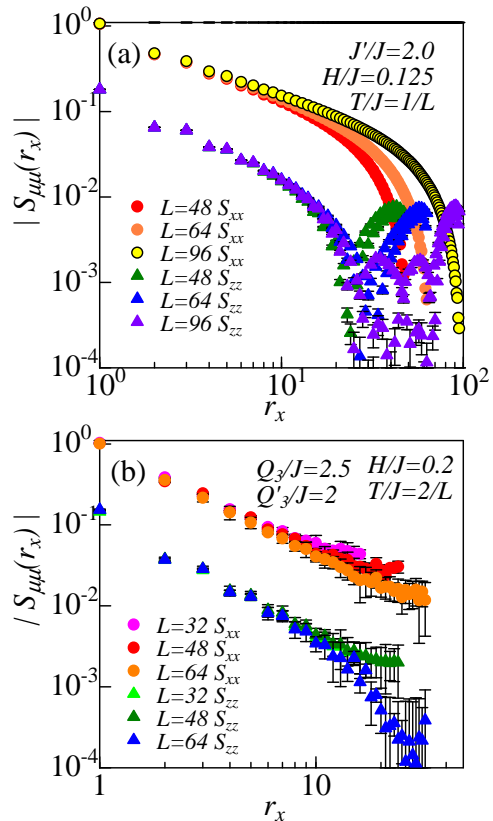


FIG. 4. (color online) Edge spin correlations $S_{\mu\mu}(r_x)$ of (a) dimerized model and (b) JQ_3 model under a magnetic field H . Circles and triangles are the transverse ($\mu = x$) and longitudinal ($\mu = z$) correlators, respectively. We have eliminated a constant part of $\langle S_j^z \rangle^2$ from the data of $\mu = z$. Like Fig. 2, we have used the normalization $S_{xx}(1) = 1$.

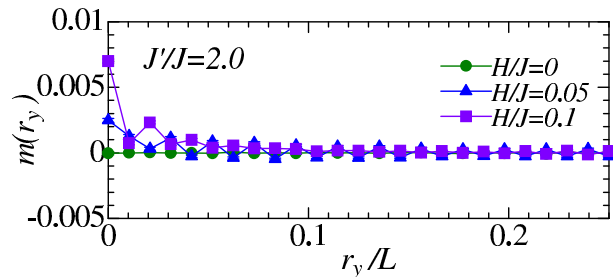


FIG. 5. (color online) Magnetization profile $m(r_y) = \langle S_{L/2, r_y}^z \rangle$ of the dimerized model with $J'/J = 2$ under magnetic fields H at $r_x = L/2$.

both extrinsically and spontaneously dimerized phases are expected to massively overlap each other.

Before the analysis, we should note the following property of the DM interaction. As we consider, for example, a uniform DM term with $\mathbf{D}_{ij} = (0, 0, D^z)$ on the bonds along the x direction [see Fig. 3(a)], the Hamiltonian $\mathcal{H}_{\text{dim}} + \mathcal{H}_{DM}$ can be mapped onto the following

easy-plane anisotropic form

$$\mathcal{H}' = \sum_j J_{\perp} (S_j^x S_{j+e_x}^x + S_j^y S_{j+e_x}^y) + JS_j^z S_{j+e_x}^z + \sum_j J(1 + \alpha \delta_{j_y, \text{even}}) \mathbf{S}_j \cdot \mathbf{S}_{j+e_y}, \quad (5)$$

via a proper unitary transformation $S_r^{\pm} \rightarrow e^{i\theta_r} S_r^{\pm}$.^{25,26} Here $J_{\perp} = J\sqrt{1 + (D^z/J)^2}$. Remarkably, the modified system (5) recovers the link-parity symmetry and has an easy-plane anisotropy. This kind of mapping can be applicable for a wide class of DM terms between neighboring spins if we adopt the open boundary condition for both x and y directions. Therefore, it is enough to study the dimerized model with an easy-plane XXZ anisotropy in order to see effects of both \mathcal{H}_{DM} and \mathcal{H}_{xxz} .

Figure 6 (a) indicates that both the longitudinal and transverse edge spin correlations decay algebraically in the system (5) with $D^z/J = 0.1$. We thus conclude that the gapless edge state is stable against both the DM and easy-plane XXZ interactions. In purely 1D spin- $\frac{1}{2}$ AF chains with easy-plane anisotropy, critical exponents $\eta_{xy,z}$ usually satisfy $\eta_z > \eta_{xy}$ in addition to $\eta_z \eta_{xy} = 1$.²² In the present 2D case of Fig. 6 (a), however, we obtain $\eta_{xy} \simeq 0.92$ and $\eta_z \simeq 1.48$. Namely, the exponents satisfy the inequality $\eta_z > \eta_{xy}$, but the relation $\eta_z \eta_{xy} = 1$ is clearly broken down. The difference between critical exponents of the 1D chain and the edge of the 2D dimerized model would be attributed to a strong correlation between bulk and edge.

The edge spin correlations for the case with $\mathcal{H}_{\text{N.N.N}}$ are given in Fig. 6 (b), in which we have adopted a ferromagnetic coupling $E/J = -0.05$ to avoid the negative sign problem. The figure shows a power-law decay of the correlation functions, and it indicates that the gapless edge mode still survives in a small $\mathcal{H}_{\text{N.N.N}}$. We, however, note that evaluated critical exponents $\eta_{xy} = \eta_z \sim 0.71$ deviate from the value of ideal TL liquid similarly to the cases with \mathcal{H}_{DM} and \mathcal{H}_{xxz} .

Figure 6 (c) is the result of the system $\mathcal{H}_{\text{dim}} + \mathcal{H}_{\text{alt}}$. As expected, the edge spin correlation changes from an algebraic form to an exponential one due to the bond dimerization along the x direction. From this analysis of perturbations, we see that the gapless nature of the edge state survives after introducing several perturbations with different symmetries except for the bond alternation \mathcal{H}_{alt} . It suggests a high possibility of the realization of a gapless edge mode in 2D spin-Peierls compounds.

V. HOW TO DETECT EDGE MODES

Finally we consider possible experimental methods of probing signatures of the gapless edge modes in 2D spin-Peierls states. As we already mentioned, a finite magnetization rapidly grows only around the edge sites as shown in Fig. 5, if we apply H in the dimerized states.

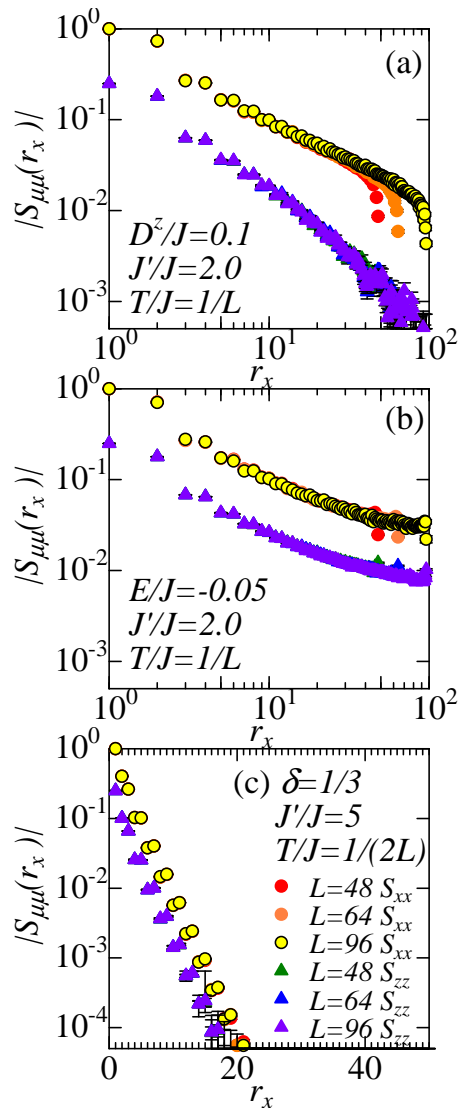


FIG. 6. (color online) Effects of (a) a DM interaction (equal to XXZ anisotropy), (b) a next-nearest neighbor interaction, and (c) an extra bond-alternation along the edge direction on the edge spin correlations of the dimerized model. Circles and triangles are the results of $\mu = x$ and $\mu = z$, respectively. In panel (c), we have used semi-log scale, and have set a larger $J'/J = 5$ and a lower temperature $T = 1/(2L)$ to depict a clear exponential-decay form of the edge correlation. In all of the panels, we have used the normalization $S_{xx}(1) = 1$.

Observing such a site-dependent magnetization (e.g., by using NMR) could indicate a signature of the existence of a gapless edge state.

The NMR relaxation rate $1/T_1$ for nuclear spins near the edge is expected to contain a power-law T dependence $T^{-\epsilon}$ at low temperatures,²² implying the existence of a gapless mode. If we assume that the dynamical critical exponent²³ z of the gapless edge state is close enough to unity, similarly to the TL liquid, we can evaluate the temperature dependence of $1/T_1$ from a simple field-theory

argument²² as follows:

$$1/T_1 = A_{xy}T^{\eta_{xy}-1} + A_zT^{\eta_z-1} + \dots, \quad (6)$$

where constants $A_{xy,z}$ depend on the strength and microscopic detail of interactions between electron and nuclear spins. This prediction of Eq. (6) indicates that critical exponents $\eta_{xy,z}$ of the edge mode can be measured from the NMR experiment in principle.

Inelastic neutron scattering spectra could also provide information about gapless edge modes. In the case of TIs, angular-resolved photoemission spectroscopy spectra^{1,2} have been often used to see the gapless dispersion on the surface and edge in addition to gapped bulk excitations. Similarly, as shown in Fig. 7, the neutron-scattering spectra are expected to possess a des Cloizeaux-Pearson-like gapless continuum^{22,27} due to the edge state in 2D Peierls magnets. As we apply a small magnetic field H , the contribution from the longitudinal spin dynamics would have a peak at an incommensurate wave number $k_x \sim \pi(1 - 2m_0)$ in which $m_0 = m(r_y = 0)$ is the magnetization on edge sites (see Fig. 5). This gapless spectra would be strong evidence for the gapless edge mode. In addition to these ways, for instance, heat transport properties would capture the nature of the gapless edge mode.

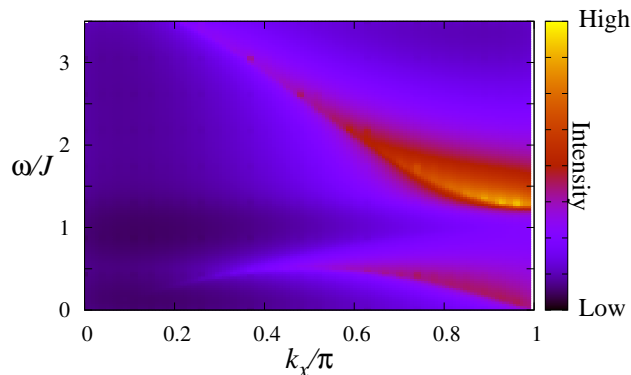


FIG. 7. (color online) Schematic inelastic-neutron-scattering spectrum of a 2D spin-Peierls phase with a gapless edge mode in the space of frequency ω and the wave number k_x . The wave number k_y is fixed to π . The weight in the low-energy region $\omega \lesssim J$ is the contribution from the edge state, which lower bound would be similar to the des Cloizeaux-Pearson mode $\sim J|\sin(k_x)|$. The weight in the higher-energy region $\omega \gtrsim J$ comes from the gapped triplet excitations in the bulk.

VI. CONCLUSIONS

We have investigated several properties of the edge spins of the dimerized and JQ_3 models, Eqs. (1a) and

(1b), by utilizing QMC simulation. The main numerical results are given in Sec. IV. When the system is in the dimerized phase and the singlet dimers do not reside on the edge, the gapless edge state really emerges. It is remarkable that the evaluated critical exponent η of the edge spin correlation becomes different from the exponent $\eta = 1$ of the usual TL liquid phases in large but finite systems at low temperatures. The deviation of η becomes larger as we approach the dimer-Néel quantum phase transition point. This non-trivial value would be caused by the strong correlation between the edge and bulk with large quantum fluctuations. In the sense of RG, the edge exponent η is naively expected to be reduced to the value of the usual TL liquid at least in the thermodynamic and zero-temperature limit, but our QMC result strongly suggests that an extremely large system size and an extremely low temperature have to be prepared in order to observe such a crossover to $\eta \rightarrow 1$. Real experiments are usually done under low but finite temperatures and magnetic crystals generally contain impurities and some kinds of defects. Therefore, the non-trivial η could be relevant and observed in real spin-Peierls materials rather than the ideal asymptotic value $\eta = 1$ of the 1D AF spin chain. The non-trivial value of η and its change depending on the “distance” from the quantum transition point are unique features of the edge state in 2D spin-Peierls phases, and they do not appear in well-studied 1D magnets such as spin ladders.

We have also shown that the edge mode is quite robust against various perturbations with different symmetries in Sec. IV B. Particularly, the stability against external magnetic field H is in contrast with the helical edge modes of TIs and free edge spins of the Haldane state, and H induces an inhomogeneous magnetization around the edge as shown in Fig. 5. The edge spin correlations algebraically decay like a TL liquid, but their critical exponents $\eta_{xy,z}$ generally violate the TL liquid relation $\eta_{xy}\eta_z = 1$, depending on the detail of the models. As expected, the deviation from the TL liquid becomes larger when coupling constants of perturbations are stronger.

We finally consider some experimental methods of detecting signatures of gapless edge modes in Sec. V. NMR, inelastic neutron scattering, and heat transport would provide hopeful experimental ways. In particular, the NMR relaxation rate $1/T_1$ has the potential to measure the value of non-trivial critical exponents $\eta_{xy,z}$ of the edge correlation.

Properties of gapless edge states we illustrate in this paper would also be useful as we study other gapless edge states of more exotic quantum spin systems. Recently, some kinds of topologically ordered states^{28,29} such as \mathbb{Z}_2 spin liquids have been predicted in relatively realistic quantum spin models, especially, frustrated models. The realization of such exotic states is generally difficult, but the comparison between their edge states and that of spin-Peierls magnets would be an interesting direction of theoretical studies in order to characterize the exotic

edge states.

ACKNOWLEDGMENT

We thank J. Lou and H. Tsunetsugu for fruitful discussions. Numerical calculations were performed at the

Institute for Solid State Physics Supercomputer Center of the University of Tokyo and cluster machines in Nano-Micro Structure Science and Engineering, University of Hyogo.

-
- ¹ M. Z. Hasan and C. L. Kane, *Rev. Mod. Phys.* **82**, 3045 (2010).
- ² X. -L. Qi and S. C. Zhang, *Rev. Mod. Phys.* **83**, 1057 (2011).
- ³ F. D. M. Haldane, *Phys. Lett. A* **93**, 464 (1983); *Phys. Rev. Lett.* **50**, 1153 (1983).
- ⁴ J. P. Renard, M. Verdaguer, L. P. Regnault, W. A. C. Erkelens, J. Rossat-Mignod and W. G. Stirling, *Europhys. Lett.* **3**, 945 (1987).
- ⁵ M. Hagiwara, K. Katsumata, Ian Affleck, B. I. Halperin, and J. P. Renard, *Phys. Rev. Lett.* **65**, 3181 (1990).
- ⁶ I. Affleck, T. Kennedy, E. H. Lieb, and H. Tasaki, *Phys. Rev. Lett.* **59**, 799 (1987); *Commun. Math. Phys.* **115**, 477 (1988).
- ⁷ M. den Nijs and K. Rommelse, *Phys. Rev. B* **40**, 4709 (1989).
- ⁸ F. Pollmann, A. M. Turner, E. Berg, and M. Oshikawa, *Phys. Rev. B* **81**, 064439 (2010).
- ⁹ Z.-C. Gu and X.-G. Wen, *Phys. Rev. B* **80**, 155131 (2009).
- ¹⁰ T. Hirano, H. Katsura, and Y. Hatsugai, *Phys. Rev. B* **77**, 094431 (2008).
- ¹¹ A. P. Schnyder, S. Ryu, A. Furusaki, and A. W. W. Ludwig, *Phys. Rev. B* **78**, 195125 (2008).
- ¹² S. Ryu, A. P. Schnyder, A. Furusaki and A. W. W. Ludwig, *New. J. Phys.* **12**, 065010 (2010).
- ¹³ A. Kitaev, *AIP Conf. Proc.* **1134**, 22 (2009).
- ¹⁴ T. Kennedy, E. H. Lieb, and H. Tasaki. *J. Stat. Phys.* **53**, 383 (1988).
- ¹⁵ N. V. Prokof'ev, B. V. Svistunov, and I. S. Tupitsyn, *Sov. Phys. JETP* **87**, 310 (1998).
- ¹⁶ O. F. Syljuåsen and A. W. Sandvik, *Phys. Rev. E* **66**, 046701 (2002).
- ¹⁷ Y. Kato, T. Suzuki, and N. Kawashima, *Phys. Rev. E* **75**, 066703 (2007).
- ¹⁸ M. Matsumoto, C. Yasuda, S. Todo, and H. Takayama, *Phys. Rev. B* **65**, 014407 (2001).
- ¹⁹ S. Wenzel and W. Janke, *Phys. Rev. B* **79**, 014410 (2009).
- ²⁰ J. Lou, A. W. Sandvik, and N. Kawashima, *Phys. Rev. B* **80**, 180414 (2009).
- ²¹ Effective theories for the Néel-dimer phase transitions have been proposed, for example, in A. Tanaka and X. Hu, *Phys. Rev. Lett.* **95**, 036402 (2005).
- ²² See, for example, T. Giamarchi, *Quantum Physics in One Dimension* (Oxford University Press, New York, 2004).
- ²³ See, for example, S. Sachdev, *Quantum Phase Transitions* (Cambridge Univ. Press, Cambridge, 1999).
- ²⁴ The dimer-Néel transition of the dimerized model is well believed to be a second-order type quantum transition. On the other hand, we should note that it is still controversial whether the dimer-Néel transition of the JQ_3 model is of a continuous type or a weak first-order type.
- ²⁵ L. Shekhtman, O. Entin-Wohlman, and A. Aharony, *Phys. Rev. Lett.* **69**, 836 (1992).
- ²⁶ See, for example, Appendix A of Ref. 8.
- ²⁷ J. des Cloizeaux, Jacques and J. J. Pearson, *Phys. Rev.* **128**, 2131 (1962).
- ²⁸ See, for example, X-G. Wen, *Quantum Field Theory of Many-Body Systems*, (Oxford univ. Press, New York, 2004).
- ²⁹ See, for example, G. Misguich and C. Lhuillier, p.229, *Frustrated Spin Systems*, Edited by H. T. Diep (World Scientific, Singapore, 2004).